X-ray Structure of Ammonia−Cellulose I: New Insights into the Conversion of Cellulose I to Cellulose III_I

Masahisa Wada,[†] Yoshiharu Nishiyama,[‡] and Paul Langan*[,§]

Department of Biomaterials Science, Graduate School of Agricultural and Life Sciences, The University of Tokyo, Tokyo 113-8657, Japan, Centre de Recherches sur les Macromolécules Végétales−CNRS, affiliated with the Joseph Fourier University of Grenoble, BP 53, 38041 Grenoble Cedex 9, France, and Bioscience Division, Los Alamos National Laboratory, Los Alamos, New Mexico 87545

Received January 30, 2006; Revised Manuscript Received March 2, 2006

ABSTRACT: A supercritical ammonia treatment has been used to trap an ammonia−cellulose complex during the conversion of cellulose I to cellulose III_I. The crystal and molecular structure of this complex, designated ammonia−cellulose I, has been determined by using X-ray fiber diffraction data (space group $P2_1$; $a = 4.47$ Å, $b = 8.81$ Å, $c = 10.34$ Å, $\gamma = 92.7°$). Although the existence of ammonia−cellulose I has been known for some time, this is the first report of its crystal structure. A one-chain monoclinic unit cell has an asymmetric unit that contains only one glucosyl residue and one ammonia molecule. The ammonia molecule acts as a bridge between hydrogen-bonded sheets, forming extended chains of cooperative hydrogen bonds. The sheets are similar to those found in cellulose III_I, with O2···O6 intrasheet hydrogen bonds and the *gt* conformation of the hydroxymethyl group providing potential bifurcated O3···O5 and O3···O6 intrachain hydrogen bonds. This new structure provides a number of insights into the structural transition pathway followed during the conversion of cellulose I to cellulose III_I.

Introduction

An important property of the linear poly(1−4) β-D glucan cellulose chain is that it can be incorporated into a number of distinct crystal phases that differ in chemical reactivity and material characteristics. Two crystal phases, I_α (one chain in space group $P1$: $a = 6.717$ Å, $b = 5.962$ Å, $c = 10.400$ Å, $\alpha = 118.08°$, $\beta = 114.80°$, and $\gamma = 80.37°$) and I_β (two parallel chains in space group $P2_1$: $a = 7.784$ Å, $b = 8.201$ Å, $c = 10.38$ Å, $\alpha = \beta = 90°$, $\gamma = 96.5°$),[1−4] are found in naturally occurring cellulose, collectively designated cellulose I, in proportions that depend on the origin of the cellulose.[5−8] The I_α phase is considered to be less stable than the I_β phase because it can be irreversibly converted to I_β by hydrothermal treatment.[9,10]

The cellulose I allomorphs can be transformed into cellulose II (two antiparallel chains in space group $P2_1$: $a = 8.10$ Å, $b = 9.03$ Å, $c = 10.31$ Å, $\alpha = \beta = 90°$, $\gamma = 117.10°$)[11,12] or cellulose III_I (one chain in space group $P2_1$: $a = 4.450$ Å, $b = 7.850$ Å, $c = 10.31$ Å, $\alpha = \beta = 90°$, $\gamma = 105.10°$)[13,14] by treatment with appropriate solvents or swelling agents. Cellulose II can be further transformed into a less well-characterized form, cellulose III_{II}.[15] Yet another phase, cellulose IV, has been reported from conversion of cellulose II or cellulose III.[16,17] A recent reinvestigation of cellulose IV suggests that, rather than corresponding to a distinct new crystal phase, it may correspond to one of the other phases with a greater amount of disorder present.[18]

Although detailed information is available on the crystal structures of I_α, I_β, II, and III_I from crystallographic,[1−4,11−14] spectroscopic,[19−22] and modeling studies,[23] less is known about the mechanisms involved in their interconversion. The processes of regeneration or caustic mercerization used to convert cellulose I to cellulose II destroys microfibrillar morphology.[24,25] In contrast, although the ammonia treatment used to convert cellulose I to cellulose III_I damages and degrades the microfibrils, their overall morphology is preserved.[26] The cellulose I ↔ cellulose III_I interconversion is essentially a solid-state reversible reaction. It may therefore be possible to characterize a structural pathway between the two phases.

Cellulose III_I is obtained from cellulose I by treatment with liquid ammonia[27−31] or various amines,[32−36] followed by removal of these reagents. The cellulose I fibers become inflated as the ammonia or amine molecules penetrate the cellulose crystallites, forming crystalline complexes with the cellulose chains. After evaporating or washing away the guest molecules, the cellulose III_I fibers look deflated and are substantially decrystallized.[37−40] These fibers can be reverse transformed into I_β by heating in water or air.[41]

We have previously reported the crystal structures of cellulose I (I_α and I_β) and cellulose III_I, determined by using a combination of X-ray and neutron fiber diffraction, ^{13}C CP/MAS NMR, and FT-IR.[3,4,13] We have also proposed a structural mechanism for the reverse transformation of cellulose III_I → cellulose I by following this transition by using in situ differential scanning calorimetry and X-ray diffraction.[41] Several crystalline amine cellulose complexes have been described by Blackwell et al.[42] In the work reported here, we have used a supercritical ammonia treatment[43] on highly oriented and crystalline cellulose I fibers[44] in order to trap an ammonia−cellulose transition complex during the conversion of cellulose I → cellulose III_I. The X-ray crystal structure of this ammonia−cellulose complex, designated ammonia−cellulose I, provides us with new insights into the structural transition pathway followed during conversion of cellulose I → cellulose III_I.

* Corresponding author. E-mail: langan_paul@lanl.gov. Telephone: 505 665 8125. Fax: 505 665 3024.

[†] Department of Biomaterials Science, Graduate School of Agricultural and Life Sciences, The University of Tokyo. E-mail: wadam@sbp.fp.a.u-tokyo.ac.jp.

[‡] Centre de Recherches sur les Macromolécules Végétales−CNRS. E-mail: yoshiharu.nishiyama@cermav.cnrs.fr.

[§] Bioscience Division, Los Alamos National Laboratory.

10.1021/ma060228s CCC: $33.50 © 2006 American Chemical Society
Published on Web 03/24/2006

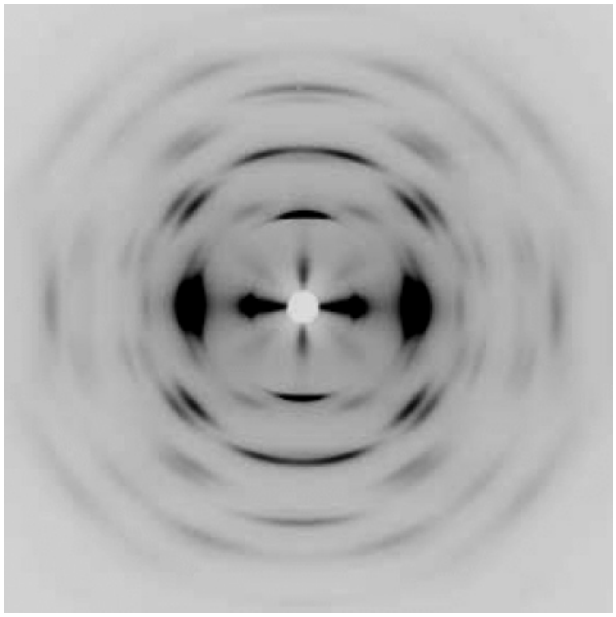

Figure 1. X-ray fiber diffraction pattern from ammonia−cellulose I recorded on a laboratory Cu K_α X-ray source.

Experimental Section

Preparation of Oriented Cellulose I Samples. Green alga *Cladophora* sp. collected at the sea of Chikura, Chiba, Japan, were used in this study. After removing calcite by boiling in 0.1 N HCl, the cellulosic algal cell walls were further purified by repetitive treatments with 5% KOH and 0.3% $NaClO_2$ aqueous solutions.[45] The purified samples were then hydrolyzed into cellulose microcrystals by a sulfuric acid treatment, followed by reconstitution into oriented films as previously reported.[44]

Conversion into Ammonia−Cellulose I. To compensate for any preferential orientation about the fiber axis within the films, the sample was bundled (thus ensuring cylindrical symmetry about the fiber axis). The bundles were then inserted into a steel pressure vessel, which was cooled in a dry ice and methanol bath. Ammonia (NH_3) gas was introduced into the cooled vessel, and the sample was immersed in liquid ammonia. The vessel was hermetically sealed and maintained at room temperature for 30 min, then heated in an oil bath at 140 °C (a few degrees over the critical temperature of ammonia, i.e., 132.5 °C) for 1 h.[13,14,43,46] After removing it from the oil bath, the vessel was cooled under tap water and the ammonia gas was leaked out. The sample was then immediately taken out of the vessel and placed in an X-ray vacuum camera for diffraction measurement. The ammonia−cellulose thus prepared was stable for several hours in a vacuum.

Data Collection and Intensity Measurement. X-ray fiber diffraction patterns were collected by using a Rigaku RU-200BH rotating anode X-ray generator (Ni-filtered Cu K_α radiation generated at 50 kV and 100 mA; $\lambda = 1.5418$ Å; 0.3 mm beam size) and a Fuji image plate (BAS-IP SR 127), Figure 1. Reflection positions were measured by using Rigaku R-Axis software and indexed by using a one-chain monoclinic lattice. The unit cell parameters were then refined by using a least-squares algorithm. The diffraction image was then transformed into reciprocal space, and the background was estimated by using an algorithm by Sonneveld and Visser[47] expanded in two dimensions. The intensity of each spot was determined by fitting a peak profile with fixed shape and a misalignment parameter by linear least-squares. A summary of the experimental parameters and the structure refinement parameters is given in Table 1. The measured observed intensity values are given in Table 2.

Structure Refinement. X-ray structure refinement was carried out by using previously described strategies for applying *SHELX-97*[48] to fiber diffraction data.[11] Atomic starting positions were taken from the chain conformation in the crystal structure of cellulose III_I.[14] A total of 38 reflections were used to refine 35 parameters with 43 applied constraints on those parameters. The data-to-parameter ratio was therefore only 2.3, significantly lower than in the refinement of other cellulose structures recently reported from synchrotron X-ray crystallographic studies, and the accuracy of the conformational parameters will be correspondingly lower.[3,4,11,14] The subsequent refinement of all atomic positions resulted in values of 25.59% and 53.35% for R and $R\omega$,[49] respectively ("parallel-up";[50] H atoms on hydroxyl groups excluded; global scaling and thermal parameters; 35 parameters and 43 restraints). A density peak in the $2F_o-F_c$ map clearly revealed the position of an ammonia molecule and incorporation of this molecule into the refinement as a single nitrogen atom resulted in values of 10.4% and 29.34% for R and $R\omega$, respectively. Refining the chains in the "parallel-down" configuration produced a significantly inferior structure.

Table 1. Experimental Details

crystal data	
chemical formula	$C_{12}H_{20}O_{10}$
cell setting, space group	monoclinic, $P2_1$
a (Å)	4.470(10)
b (Å)	8.810(13)
c (Å)	10.340(19)
α (deg)	90
β (deg)	90
γ (deg)	92.7(2)
data collection	
λ (Å)	1.5418
independent reflections	38
reflections > $2\sigma(I)$	27
θ_{max} (deg)	11.08
range of h	0 → 2
range of k	−4 → 4
range of l	−5 → 5
refinement	
refinement on	F^2
$R[F^2 > 2\sigma(F^2)]$	0.1040
$\omega R(F^2)$	0.2934

The coordinates of the final structure are given in Table 3 and represented in Figure 2. Selected conformational features of ammonia−cellulose I and other cellulose allomorphs are given in Table 4. Interatomic distances and angles of interest, including those of possible hydrogen bonds in ammonia−cellulose I, are represented in Table 5. Two over-short contacts were present in the final structure between H5 and H6B (2.12 Å) and between H4 and H3 (2.31 Å). Because these contacts involved only H atoms that ride on C atoms during refinement, we decided not to try to relieve the distances of 0.28 and 0.09 Å by using repulsive constraints.

Results and Discussion

The relative orientation of adjacent glucosyl residues can be described by the glycosidic torsion angles Φ and Ψ and the bond angle τ, and the conformation of hydroxymethyl groups can be described by torsion angles χ and χ'. The conformational parameters of ammonia−cellulose I are similar to those found in cellulose II and cellulose III_I, Table 4. There are three low-energy conformations for the hydroxymethyl group in cellulose, designated *tg*, *gg*, and *gt*; the first letter indicates whether the position of the O6 atom is either trans or gauche with respect to atom O5, and the second refers to its position with respect to atom O4. The hydroxymethyl group is *gt* in ammonia−cellulose I, as it is in cellulose II and III_I, whereas it is *tg* in cellulose I_α and I_β.

The chains pack in a distinctly different way in ammonia−cellulose I, Figure 3. Parallel chains are arranged edge-to-edge in flat sheets that stack on top of one another in cellulose I_α and I_β, Figure 3 (top). Within each sheet, neighboring chains interact through O−H···O hydrogen bonds, but there are no such hydrogen bonds between the stacked sheets, only weaker

Table 2. Measured Observed Intensity Values, where *h*, *k*, and *l* are Miller Indices, *I* is Intensity, σ_I is the Error in Intensity, and *m* is the Multiplicity of Each Reflection[a]

h	*k*	*l*	*I*	σ_I	*m*	*h*	*k*	*l*	*I*	σ_I	*m*	*h*	*k*	*l*	*I*	σ_I	*m*
0	1	0	24.84	7.04	2	2	0	1	0.00	0.00	−2	0	0	3	1.26	1.12	2
1	0	0	0.00	0.00	−2	0	4	1	8.64	2.94	2	0	1	3	9.46	4.34	2
0	2	0	144.00	12.00	2	2	−1	1	0.00	0.00	−2	1	0	3	0.00	0.00	−2
1	−1	0	0.00	0.00	−2	2	1	1	5.03	2.24	2	0	2	3	8.67	2.94	2
1	1	0	126.25	5.12	2	0	0	2	5.03	2.24	1	1	−1	3	0.00	0.00	−2
1	−2	0	1.00	0.50	2	0	1	2	2.58	1.60	2	1	1	3	12.09	3.48	2
1	−3	0	0.5	0.5	2	1	0	2	0.00	0.00	−2	1	−2	3	2.39	1.54	2
2	0	0	0.00	0.00	−2	0	2	2	35.63	5.97	2	1	2	3	3.91	1.98	2
0	4	0	9.14	3.02	2	1	−1	2	0.00	0.00	−2	0	3	3	8.60	2.07	2
0	0	1	0.08	0.08	1	1	1	2	30.08	5.48	2	1	−3	3	0.0	0.0	−2
0	1	1	0.03	0.03	2	1	−2	2	2.36	1.54	2	1	3	3	11.49	3.39	2
1	0	1	0.00	0.00	−2	1	2	2	2.04	1.43	2	0	0	4	9.31	3.05	1
0	2	1	16.74	4.09	2	0	3	2	2.48	2.22	2	1	0	4	0.00	0.00	−2
1	−1	1	0.00	0.00	−2	1	−3	2	2.87	1.69	2	0	2	4	6.92	2.63	2
1	1	1	7.11	2.67	2	1	3	2	3.14	1.77	2	1	−1	4	0.00	0.00	−2
1	−2	1	9.07	3.01	2	2	0	2	0.00	0.00	−2	1	1	4	4.66	2.16	2
1	2	1	5.00	2.24	2	0	4	2	9.34	3.06	2	1	−2	4	0.00	0.0	−2
0	3	1	8.14	4.04	2	2	−1	2	0.00	0.00	−2	1	2	4	3.26	1.81	2
1	−3	1	10.82	3.29	2	1	−4	2	5.62	2.37	2						
1	3	1	8.14	2.85	2												

[a] A negative multiplicity indicates that the intensity of this reflection is included in the intensity of the following reflection as an overlapping composite intensity.

Table 3. Fractional Atomic Coordinates of the Atoms for One Glucosyl Residue of the Chain of Ammonia−Cellulose I[a]

atom	*x*	*y*	*z*
C1	0.000(11)	0.047(4)	0.9994(11)
H1	−0.2112	0.0125	1.0065
C2	0.025(15)	0.177(3)	0.906(2)
H2	0.2357	0.2137	0.9024
C3	−0.070(17)	0.128(4)	0.772(2)
H3	−0.2896	0.1180	0.7694
C4	0.053(14)	−0.022(3)	0.7314(11)
H4	0.2644	−0.0053	0.7080
C5	0.030(13)	−0.140(3)	0.8381(19)
H5	−0.1822	−0.1636	0.8566
O5	0.171(11)	−0.075(4)	0.953(2)
O2	−0.15(2)	0.299(5)	0.950(4)
O3	0.03(3)	0.246(5)	0.684(4)
O4	−0.106(12)	−0.087(4)	0.6212(16)
C6	0.179(19)	−0.284(4)	0.810(3)
H6A	0.1157	−0.3217	0.7253
H6B	0.3944	−0.2647	0.8073
O6	0.11(2)	−0.396(5)	0.905(8)
N1	−0.501(19)	−0.543(7)	0.603(10)

[a] The global isotropic atomic thermal displacement parameter is 0.16.

interactions such as C−H···O. The main difference between cellulose I_α and I_β is in the relative stagger of these sheets in the chain direction.[3,4] Accommodating the ammonia molecules in ammonia−cellulose I shifts the stacked sheets from their relative position in cellulose I in two directions; the sheets are shifted in the chain axis direction so that stacked sheets are no longer staggered with respect to each other, and the sheets are also sheared perpendicular to the chain axis, in the direction indicated by the red arrow in Figure 3 (middle), so that the sugar rings of chains in neighboring sheets no longer partially overlap and interact through C−H···O interactions, but rather the sugar rings pack directly on top of each other in hydrophobic stacks as in cellulose III_I, Figure 3 (bottom).

Within the sheets, the interchain hydrogen bonds are mostly between O2 and O6 atoms in ammonia−cellulose I and cellulose III_I and, because of the difference in hydroxymethyl group orientation, between O6 and O3 atoms in cellulose I. It is not possible to assign with confidence hydrogen bond donor and acceptor roles in ammonia−cellulose I because hydrogen atoms could not be directly located. However, we note that the angles of 116(5)° and 145(5)° for the C2−O2···O6 and C6−O6···O2 geometries, respectively, would result in a more linear hydrogen bond if O2 is the donor.

Each ammonia molecule in ammonia−cellulose I sits in a distorted box defined by the edges of four neighboring chains, as shown in Figure 4. The atoms at the vertexes of this box are the six oxygen atoms O3, O3′, O6, O6′, O2, O2′, and the two aliphatic hydrogen atoms H6A, H6A′, where a prime after the atom symbol indicates that the atom's chain is in a neighboring sheet. Four of these oxygen atoms, O3, O3′, O6, and O2′, are close enough to potentially hydrogen bond with the ammonia molecule, Table 5. The O3, O3′ atoms also have the potential to donate an intrachain hydrogen bond to the oxygen O5 ring atom of the next glucose residue as observed previously for cellulose I_α, cellulose I_β, cellulose II, and cellulose III_I.[3,4,11−13] They also have the potential to donate to the O6 atom of the next glucose residue in a bifurcated arrangement, as previously observed for cellulose II and cellulose III_I[11−13] and, indeed, for all β-1,4-linked hydroxylated small molecules that have a 2-fold screw axis and O6 in the *gt* conformation.[51] This observation, and also the fact that each O3 atom interacts with two ammonia molecules, one on either side of its sheet, suggests that the O3 atoms accept hydrogen bonds from the ammonia molecules. The O3 atoms and the ammonia molecules are therefore connected in an extended zigzag chain of hydrogen bonds running perpendicular to the chain axis and bridging the stacked sheets, as shown by the dashed green lines in Figure 2.

The angles of 122(6)° and 168(4)° for the C6−O6···N and C2−O2···N geometries in ammonia−cellulose I would result in a more linear hydrogen bond if O6 is donor and O2 is acceptor, agreeing with O2 as donor in the intrasheet hydrogen bond. However, the geometrical arrangement of the O atoms within hydrogen-bonding distance of the ammonia molecule (O3, O3′, O2′, and O6) is far from ideal for tetrahedral coordination, and it is possible that there are bifurcated hydrogen bonds present or that the orientation of the ammonia molecules has a certain amount of disorder. With no direct information on hydrogen atom positions, it is not even possible to say whether the O3 and O3′ atoms each accept a single hydrogen bond from a bridging ammonia molecule (the O3′···N···O3 angle of 95(3)° almost matches a H−N−H angle of ∼106°) or whether the bridging ammonia molecule donates a single bifurcated hydrogen bond to O3 and O3′. However, although

CDV

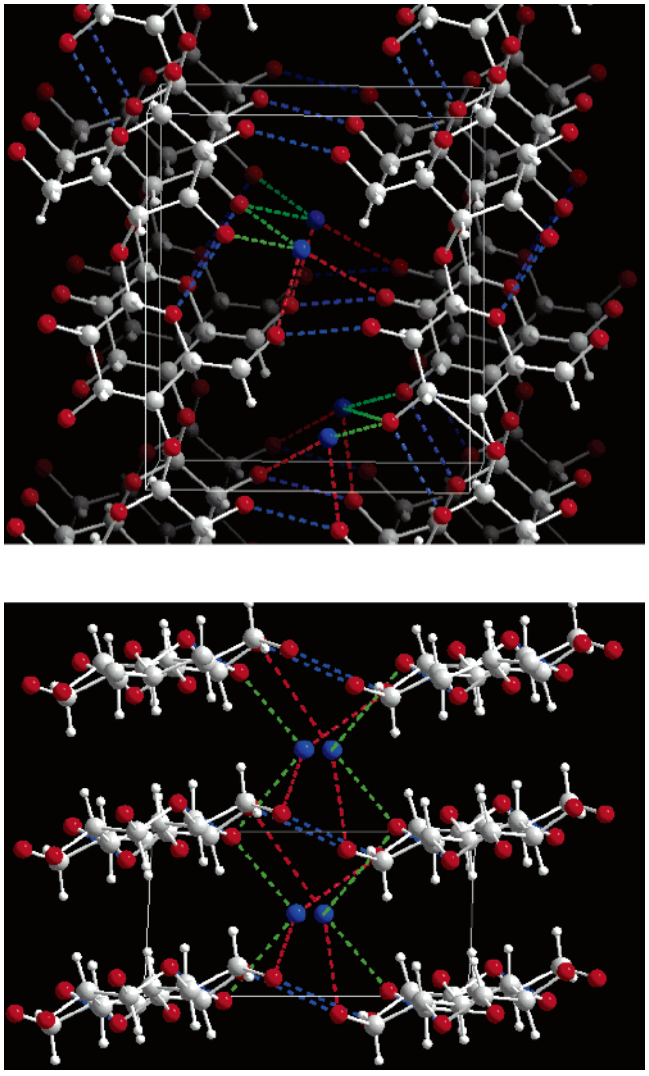

Figure 2. Crystal structure of ammonia−cellulose I; (top) viewed perpendicular to the *c* axis direction (the chain direction) with the *c* axis tilted slightly to show the zigzag extended network of intersheet O3···N···O3 hydrogen bonds (green dashed lines), potential O6···N and O2···N ammonia bridge hydrogen bonds (red dashed lines), and the intrachain O3···O5 and intrasheet O2···O6 hydrogen bonds (blue dashed lines); (bottom) viewed in projection down the *c* axis direction: C, O, N, and H atoms are represented as gray, red, blue, and white balls, respectively. Covalent and hydrogen bonds are represented as full and dashed sticks, respectively.

there is little we can say about the exact hydrogen-bonding arrangement, and despite the possibility of disorder between the donor/acceptor roles of O2 and O6, it is clear that an extended zigzag network of O3···N···O3′ hydrogen bonds exists.

The ammonia molecule acts as a bridge between hydrogen-bonded sheets, Figures 2 and 3. On evaporation of ammonia, the 4.4 Å long (O6···N···O2) ammonia bridge in ammonia−cellulose I is broken, and a ∼2.2 Å displacement along the direction of the red arrow in Figure 3 (middle) (approximately the direction of the *b* axes) in combination with a small change in chain orientation, brings the two chains at either end of the long diagonal of the unit cell into position to form a 2.6 Å long intersheet O6−H···O2 hydrogen bond, thus generating the unit cell of cellulose III_I. Hydrogen-bonded (O2−H···O6) sheets are not disrupted in going from ammonia−cellulose I to cellulose III_I, only their relative displacement changes, Figure 3.

With the alternative choice of unit cell for cellulose III_I represented in yellow in Figure 3 (a = 4.45 Å, b = 7.85 Å, c = 10.31 Å, γ = 76.9°), it can be seen that the conversion from ammonia−cellulose I to cellulose III_I corresponds essentially to the stacked sheets shearing in the *b* axis direction so that the value of γ decreases from 92° to 76.9° with a corresponding shrinkage in the size of the long *b* axis from 8.81 to 7.85 Å. The sizes of the *a* and *c* axes remain relatively unchanged. These changes in γ and *b* correspond to a decrease in unit cell volume from 406.9 to 347.7 Å^3. In going from cellulose I to ammonia−cellulose I, the unit cell volume, per chain, increases from about 329 to 406.9 Å^3. The penetration of an ammonia molecule therefore causes the unit cell of cellulose to swell by around 30 Å^3.

There is conceivably another pathway from ammonia−cellulose I to cellulose III_I. On evaporation of ammonia, if the two chains at opposite ends of the short diagonal of the ammonia−cellulose I unit cell are displaced by ∼1.6 Å and then rotated by ∼30°, the O2 and O6 atoms of these chains would be brought into hydrogen-bonding distance. In this case the initial distance between these O2 and O6 atoms is ∼6 Å, i.e., larger than in the former case. This path would also involve a rearrangement of the hydrogen-bonded sheets.

In summary, the crystal structure presented here is the first for ammonia−cellulose I, and when compared to those previously reported for cellulose I and III_I, provides the following insights into the conversion of cellulose I → cellulose III_I. Cellulose I consists of hydrogen-bonded sheets that stack on top of each other through C−H···O and van der Waals interactions. Ammonia molecules penetrate between these sheets, lubricating them and causing them to slide over each other. The ammonia molecules can be accommodated at specific

Table 4. Selected Conformational Parameters of Ammonia−Cellulose I Compared with Those of the Other Cellulose Allomorphs[a]

	Φ	Ψ	τ	χ	χ′	θ
ammonia−cellulose I	−96	90	117	69	−171	15.1
cellulose III_I	−92	93	116	44	163	10.5
cellulose II origin	−97	95	116	72	−165	5.0
cellulose II center	−94	87	115	58	−175	10.2
cellulose I_α upper residue	−99	94.6	116	166	−74	6.9
cellulose I_α lower residue	−98	99.2	116	167	−75	9.4
cellulose I_β origin	−98.5	90.5	115	170	−70	10.2
cellulose I_β center	−88.7	94.5	116	158	−83	6.7

[a] The conformation of the hydroxymethyl group is defined by two letters, the first referring to the torsion angle χ (O5−C5−C6−O6) and the second to the torsion angle χ′ (C4−C5−C6−O6). Thus the ideal *tg* and *gt* conformations would be respectively defined as sets of two angles (180°, 60°) and (60°, 180°). The glycosidic bond angle, τ, is defined by (C1−O4−C4). The glycosidic torsion angles Φ and Ψ, which describe the relative orientation of adjacent glucosyl residues in the same chain, are defined by (O5−C1−O1−C4) and (C1−O1−C4−C3), respectively. The sugar pucker parameter θ is defined as in Cremer, D.; Pople, J. *J. Am Chem Soc*. **1975**, *97*, 1354−1358.

Table 5. Interatomic Distances (Å) and Angles (deg) of Potential Hydrogen Bonds of interest.

intramolecular	
O3···O5	2.94(6)
O3···O6	3.25(7)
intermolecular	
O6···O2	2.91(7)
N1···O3	3.19(13)
N1···O3′	2.86(13)
N1···O2′	3.14(10)
N1···H6A	2.9414
N1···O6	2.76(13)
C6 −O6···O2	145(5)
C2−O2···O6	116(5)
C6−O6···N	122(6)
C2−O2···N	168(4)

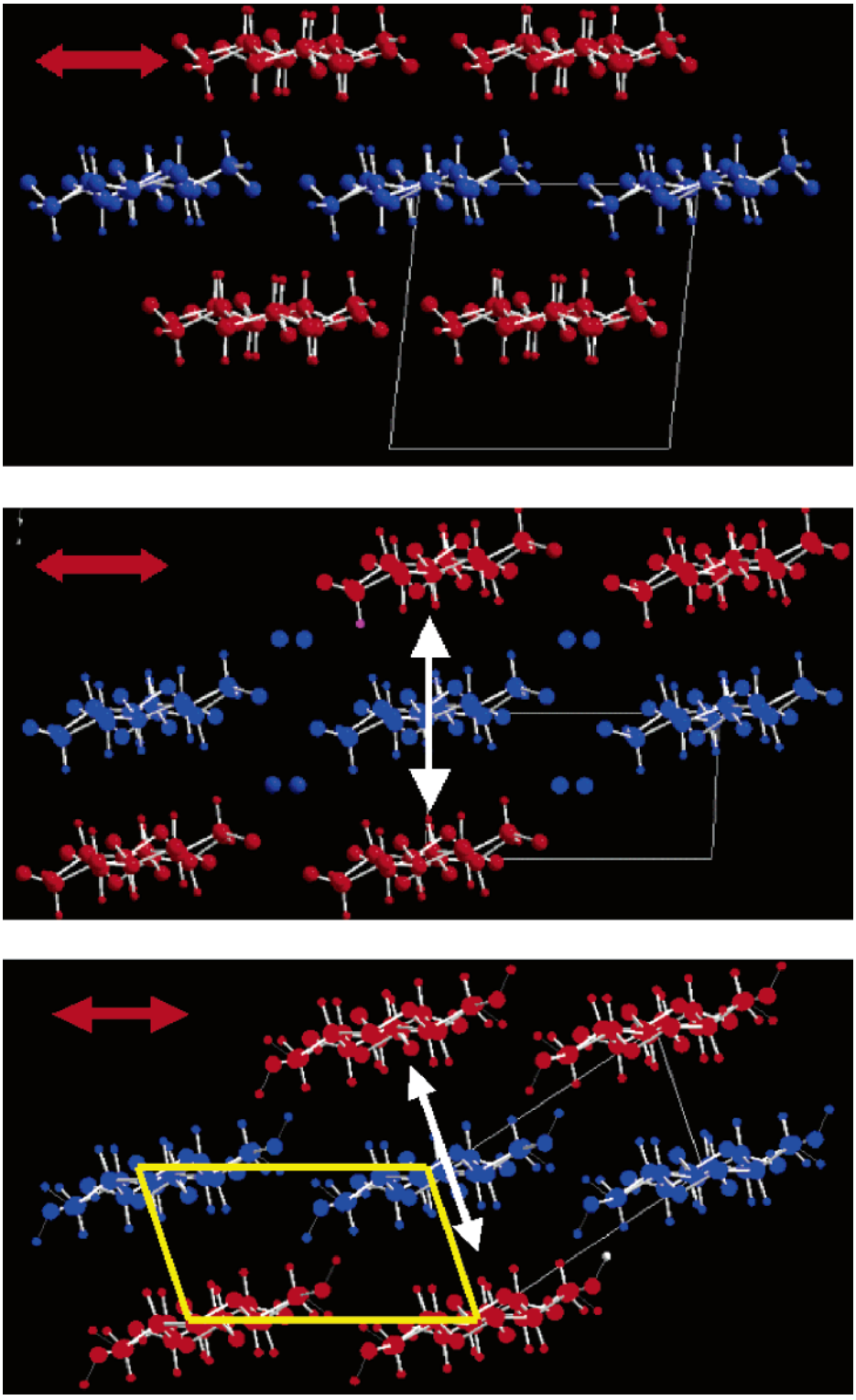

Figure 3. Projections of the crystal structures of cellulose I, ammonia−cellulose I, and cellulose III_I with the stacked hydrogen-bonded sheets represented in different colors. The crystallographic unit cells are represented by thin white lines. Red arrows indicate the direction of sheet slippage during the structural transition from cellulose I → ammonia−cellulose I → cellulose III_I. The white arrows indicate the hydrophobic stacking direction of chains in ammonia−cellulose I and cellulose III_I. An alternative choice of unit cell for cellulose III_I is represented in yellow for the purposes of simplifying the discussion of the conversion mechanism.

and regular sites between the sheets if the hydroxymethyl groups change rotation from *tg* to *gt*. The ammonia molecules form hydrogen bond bridges between sheets, replacing the C−H···O intersheet interactions found in cellulose I. When the ammonia molecules evaporate, the ammonia bridge is replaced by an intersheet O−H···O hydrogen bond with small changes in relative chain displacement and orientation. We note that the hydrophobic stacking of chains, indicated by the white arrows in Figure 3 (middle and bottom), would not be disrupted by a relatively small sheet slippage in going from ammonia−cellulose I → cellulose III_I.

Hydrogen-bonded sheets persist throughout the transition from cellulose I → ammonia−cellulose I → cellulose III_I and the reverse transition from cellulose III_I → cellulose I; it is only

CDV

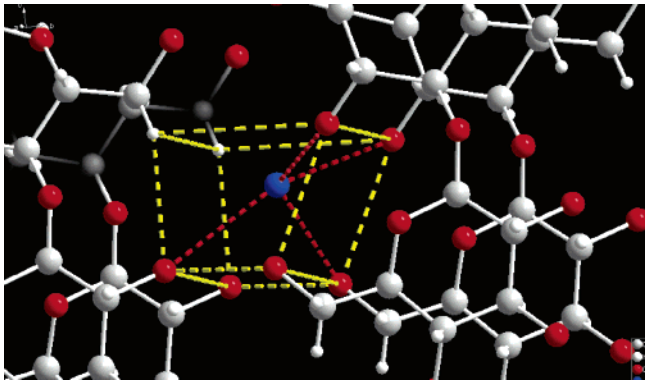

Figure 4. Detail of the crystal structure of ammonia−cellulose I showing the local environment of the ammonia molecule. Each N atom sits in a skewed box (yellow dashed lines) defined by atoms O3, O3′, O6, O6′, O2, O2′, H6A, and H6A′. O atoms that are within hydrogen-bonding distance of N are connected to N by a red dashed line. C, O, N, and H atoms are represented as gray, red, blue, and white balls, respectively. Covalent and hydrogen bonds are represented as full and dashed sticks, respectively.

their relative displacement and their stacking interactions that change. Interestingly, both ammonia−cellulose I and cellulose III_I have stacking interactions that involve extended zigzag chains of hydrogen bonds perpendicular to the chain directions. These types of arrangements will be particularly strong because of their cooperative nature. However, this cooperative nature may also lead to a susceptibility to rapid or discontinuous change; breaking a few intersheet hydrogen bonds in ammonia−cellulose I or cellulose III_I may completely destabilize these phases.

Acknowledgment. P.L. thanks the Office of Science and the Office of Biological and Environmental Research of the U.S. Department of Energy for financial support.

References and Notes

(1) Sugiyama, J.; Vuong, R.; Chanzy, H. *Macromolecules* **1991**, *24*, 4168−4175.
(2) Sugiyama, J.; Okano, T.; Yamamoto, H.; Horii, F. J. *Macromolecules* **1990**, *23*, 3196−3198.
(3) Nishiyama, Y., Sugiyama, J., Chanzy, H., Langan, P. *J. Am. Chem. Soc.* **2003**, *125*, 14300−14306.
(4) Nishiyama, Y.; Langan, P.; Chanzy, H. *J. Am. Chem. Soc*. **2002**, *124*, 9074−9082.
(5) Atalla, R. H.; VanderHart, D. L. *Science* **1984**, *223*, 283−285.
(6) Horii, F.; Hirai, A.; Kitamaru, R. *Macromolecules* **1987**, *20*, 2117−2120. (These authors refer to I_α and I_β to distinguish respectively the ramie and cotton family from that of *Valonia* and bacterial cellulose).
(7) Belton, P. S.; Tanner, S. F.; Cartier, N.; Chanzy, H. *Macromolecules* **1989**, *22*, 1615−1617.
(8) Larsson, P. T.; Westmark, U.; Iverson, T. *Carbohydr. Res.* **1995**, *278*, 339−343.
(9) Horii, F.; Yamamoto, H.; Kitamaru, R.; Tanahashi, M.; Higuchi, T. *Macromolecules* **1987**, *20*, 2946−2949.
(10) Yamamoto, H.; Horii, F.; Odani, H. *Macromolecules* **1989**, *22*, 4130−4132.
(11) Langan, P.; Nishiyama, Y.; Chanzy, H. *Biomacromolecules* **2001**, *2*, 410−416.
(12) Langan, P.; Nishiyama, Y.; Chanzy, H. *J. Am. Chem. Soc*. **1999**, *121*, 9940−9946.
(13) Wada, M.; Heux, L.; Isogai, A.; Nishiyama, Y.; Chanzy, H.; Sugiyama, J. *Macromolecules* **2001**, *34*, 1237−1243.
(14) Wada, M.; Chanzy, H.; Nishiyama, Y.; Langan, P. *Macromolecules* **2004**, *37*, 8548−8555.
(15) Sarko, A.; Southwick, J.; Hayashi, J. *Macromolecules* **1976**, *9*, 857−863.
(16) Hutino, K.; Sakurada, I. *Naturwissenschaften* **1940**, *28*, 577−578.
(17) Kulshreshtha, A. K. *J. Text. Inst.* **1979**, *1*, 13−18.
(18) Wada, M.; Heux, L.; Sugiyama, J. *Biomacromolecules* **2004**, *5*, 1385−1391.
(19) Kono, H.; Yunoki, S.; Shikano, T.; Fujiwara, M.; Erata, T.; Takai, M. *J. Am. Chem. Soc.* **2002**, *124*, 7506−7511.
(20) Kono, H.; Numata, Y. *Polymer* **2004**, *45*, 4541−4547.
(21) Kono, H.; Erata, T.; Takai, M. *Macromolecules* **2003**, *36*, 3589−3592.
(22) Kono, H.; Numata, Y.; Erata, T.; Takai, M. *Macromolecules* **2004**, *37*, 5310−5316.
(23) Ford, Z. M.; Stevens, E. D.; Johnson, G. P.; French, A. D. *Carbohydr. Res.* **2005**, *340*, 827−833.
(24) Dinand, E.; Vignon, M.; Chanzy, H.; Heux, L. *Cellulose (Dordrecht, Neth.)* **2002**, *9*, 7−18.
(25) Shibazaki, H.; Kuga, S.; Okano, T. *Cellulose (Dordrecht, Neth.)* **1997**, *4*, 75−87.
(26) Chanzy, H.; Henrissat, B.; Vincendon, M.; Tanner, S. F.; Belton, P. S. *Carbohydr. Res.* **1987**, *160*, 1−11.
(27) Hess, K.; Trogus, C. *Ber. Dtsch. Chem. Ges. B* **1935**, *68*, 1986−1988.
(28) Barry, A. J.; Peterson, F. C.; King, A. J. *J. Am. Chem Soc*. **1936**, *58*, 333−337.
(29) Clark, G. L.; Parker, E. A. *J. Phys. Chem*. **1937**, *41*, 777−786.
(30) Hess, K.; Gundermann, J. *Ber. Dtsch. Chem. Ges. B* **1937**, *70*, 1788−1790.
(31) Legrand, C. *J. Polym. Sci.* **1951**, *7*, 333−339.
(32) Trogus, C.; Hess, K. *Z. Phys. Chem. Abt. B* **1931**, *14*, 387−395.
(33) Davis, W. E.; Barry, A. J.; Peterson, F. C.; King, A. J. *J. Am. Chem. Soc*. **1943**, *65*, 1294−1299.
(34) Loeb, L.; Segal, L. *J. Polym. Sci*. **1955**, *15*, 343−354.
(35) Creely, J. J.; Wade, R. H. *Text. Res. J*. **1975**, *45*, 240−246.
(36) Creely, J. J.; Wade, R. H. *J. Polym. Sci.: Polym. Lett. Ed*. **1978**, *16*, 291−295.
(37) Chanzy, H.; Henrissat, B.; Vuong, R.; Revol, J.-F. *Holzforschung* **1986**, *40 Suppl.*, 25−30.
(38) Sugiyama, J.; Harada, H.; Saiki, H. *Int. J. Biol. Macromol*. **1987**, *9*, 122−130.
(39) Lewin, M.; Roldan, L. G. *J. Polym. Sci., Part C* **1971**, *36*, 213−229.
(40) Rousselle, M.-A.; Nelson, M. L. *Text. Res. J*. **1976**, *46*, 648−653.
(41) Wada, M. *Macromolecules* **2001**, *34*, 3271−3275.
(42) Blackwell, J.; Kurz, D.; Su, M.; Lee, D. M. In *ACS Symp. Ser*. **1987**, *340*, 199−213.
(43) Yatsu, L. Y.; Calamari, T. A.; Benerito, R. R. *Text. Res. J*. **1986**, *56*, 419−424.
(44) Nishiyama, Y.; Kuga, S.; Wada, M.; Okano, T. *Macromolecules* **1997**, *30*, 6395−6397.
(45) Sugiyama, J.; Persson, J.; Chanzy, H. *Macromolecules* **1991**, *24*, 2461−2466.
(46) Isogai, A.; Usuda, M.; Kato, T.; Uryu, T.; Atalla, R. H. *Macromolecules* **1989**, *22*, 3168−3172.
(47) Sonneveld, E. J.; Visser, J. W. *J. Appl. Crystallogr.* **1975**, *8*, 1−7.
(48) Sheldrick, G. M. *SHELX-97, A Program for the Refinement of Single-Crystal Diffraction Data*; University of Gottingen: Gottingen, Germany, 1997.
(49) R is calculated from $\Sigma(|Fo| - |Fc|)/\Sigma|Fo|$ with $Fo > 4\sigma$, where Fo and Fc are the observed and calculated amplitudes, respectively. $R\omega$ is calculated from $[\Sigma\omega(Fo^2 - Fc^2)^2/\Sigma\omega(Fo^2)^2]^{1/2}$, where ω is a weight $(1/\sigma^2)$ applied to each F^2 term in the least squares refinement. $R\omega$ will be more than twice the size of the R.
(50) The "parallel-up" and "parallel-down" structures are defined according to the definition of French, A. D. and Howley, P. D. in *Cellulose and Wood, Chemistry and Technology*; Schuerch, C., Ed.; Wiley: New York, 1989, p 164.
(51) Peralta-Inga, Z.; Johnson, G. P.; Dowd, M. K.; Rendleman, J. A.; Stevens, E. D.; French, A. D. *Carbohydr. Res.* **2002**, *337*, 851−861.

MA060228S